Support Information

Influence of Pt/ionomer/water interface on oxygen reduction reaction: Insights for micro-three-phase interface

Shangkun Jiang[# a, b, c], *Qiong Xiang*[# a, b], *Zhuoyang Xie* [a, b], *Na Yang* [d], *Jiawei Liu* [e], *Li Li* [a, b]*, *and Zidong Wei* [a, b]*

[a]State Key Laboratory of Advanced Chemical Power Sources (Chongqing University)

[b]School of Chemistry and Chemical Engineering, Chongqing University, Chongqing, 400044, China.

[c]College of Chemistry and Chemical Engineering, Chongqing University of Science &Technology, Chongqing, 401331, China

[d]School of Materials and Energy, University of Electronic Science and Technology of China, Chengdu, 611731, China

[e]Institute of Sustainability for Chemicals, Energy and Environment (ISCE2), Agency for Science, Technology and Research (A*STAR), 627833, Singapore

* Corresponding authors

E-mail addresses: liliracial@cqu.edu.cn (L. Li); zdwei@cqu.edu.cn (Z. Wei)

[#] These authors contributed equally to this work.

Contents

S1. Micro kinetics of oxygen reduction reaction 2

S2. The computational details of slow growth.....4

S3. The structure of Pt/ionomer/water interface 4

S4. The electric double layer structure of Pt/ionomer/water interface 6

S5. The ORR activity of Pt/ionomer/water interface.....9

Reference 14

S1. Micro kinetics of oxygen reduction reaction

Calculating the free energy of reactions is crucial for understanding and predicting the feasibility and dynamics of reactions. It involves using quantum chemical methods to estimate the change in free energy of a reaction at a specific potential, thus predicting the rate and direction of the reaction. Nørskov et al. [1] employ a general kinetic model for the oxygen reduction reaction motivated by previous DFT calculations without a priori assumptions about rate-determining steps. In this model, O_2 molecules diffuse from the bulk electrolyte to the catalyst-electrolyte interface, given by,

$$O_2(aq) \underset{k_{-1}}{\overset{k_1}{\rightleftharpoons}} O_2(dl) \tag{1}$$

O_2 may then adsorb on free lattice sites and participate in the hydrogen bonded network and this is given by

$$O_2(dl) + *_A \underset{k_{-2}}{\overset{k_2}{\rightleftharpoons}} O_2*_A \tag{2}$$

Once adsorbed on the surface, O_2 can be reduced to H_2O by a series of proton-coupled electron transfer steps in the associative pathway[2]

$$O_2*_A + H^+ + e^- \underset{k_{-3}}{\overset{k_3}{\rightleftharpoons}} OOH*_A \tag{3}$$

$$OOH*_A + H^+ + e^- \underset{k_{-4}}{\overset{k_4}{\rightleftharpoons}} O*_A + H_2O \tag{4}$$

$$O*_A + H^+ + e^- \underset{k_{-5}}{\overset{k_5}{\rightleftharpoons}} OH*_A \tag{5}$$

$$OH*_A + H^+ + e^- \underset{k_{-6}}{\overset{k_6}{\rightleftharpoons}} *_A + H_2O \tag{6}$$

According to transition state theory, the rate constant is given by

$$k_i = \frac{k_B T}{h} \exp\left(-\frac{G_{a,i}}{k_B T}\right) \tag{7}$$

Where $G_{a,i}$ is the activation free energy. For chemical dissociation steps, we neglect the activation entropy and use activation energies calculated by Tripkovic et al. [3] for the solvated Pt(111) surface. We use Brønsted−Evans−Polanyi (BEP) relations derived from previously published DFT calculations to describe variations in the activation free energy with variations in the dissociation free energy relative to platinum. [4, 5] With these approximations, the activation free energy is given by

$$G_{a,i} \approx E_{a,i}^{Pt} + \gamma_i\left(\Delta G_i - \Delta G_i^{Pt}\right) \tag{8}$$

where $E_{a,i}^{Pt}$ is the activation energy on Pt(111), $\Delta G_i - \Delta G_i^{Pt}$ is the reaction free energy of the step relative to Pt(111), and γ_i is the BEP slope. The rate constants of an electrochemical reduction step, *i*, is assumed to take the functional form

$$k_i = \frac{k_B T}{h}\exp\left(-\frac{G_{a,i}^0}{k_B T}\right)\exp\left(-\frac{e\beta_i\left(U - U_i^0\right)}{k_B T}\right) \quad (9)$$

where $G_{a,i}^0$ is the activation free energy at the reversible potential of the step, U_i^0. The reversible potential of step *i*

$$U_i^0 = -\frac{\Delta G_i^0}{e} \quad (10)$$

The rate equations for elementary reactions of ORR displayed as eq (1-6) are shown as following:

$$r_1 = k_1 x_{O_2(aq)} - k_{-1} x_{O_2(dl)} \quad (11)$$

$$r_2 = k_2 x_{O_2(dl)} \theta_{*A} - k_{-2} \theta_{O_2*A} \quad (12)$$

$$r_3 = k_3 \theta_{O_2*A} - k_{-3} \theta_{OOH*A} \quad (13)$$

$$r_4 = k_4 \theta_{OOH*A} - k_{-4} x_{H_2O} \theta_{O*A} \quad (14)$$

$$r_5 = k_5 \theta_{O*A} - k_{-5} \theta_{OH*A} \quad (15)$$

$$r_6 = k_6 \theta_{OH*A} - k_{-6} x_{H_2O} \theta_{*A} \quad (16)$$

Where θ denotes the surface coverage of the intermediate species during the ORR process. The $x_{O_2(aq)}$ and x_{H_2O} were set as 2.3×10^{-5} and 1, respectively, to simulate their saturated concentration during water solvent. Assuming that all the intermediate species are in steady state during ORR process, one could obtain the relationship between coverage of species and potential can be obtained by save the equations as follows:

$$\frac{\partial x_{O_2(dl)}}{\partial t} = r_1 - r_2 = 0 \quad (17)$$

$$\frac{\partial \theta_{O_2*A}}{\partial t} = r_2 - r_3 = 0 \quad (18)$$

$$\frac{\partial \theta_{OOH*A}}{\partial t} = r_3 - r_4 = 0 \quad (19)$$

$$\frac{\partial \theta_{O*A}}{\partial t} = r_4 - r_5 = 0 \quad (20)$$

$$\frac{\partial \theta_{OH*A}}{\partial t} = r_5 - r_6 = 0 \quad (21)$$

$$\frac{\partial \theta_{*_A}}{\partial t} = r_6 - r_2 = 0 \quad (22)$$

$$\sum_{i=species} \frac{\partial \theta_i}{\partial t} = 1 \quad (23)$$

The ORR polarization curve is available to be calculated via:

$$j = -4e\rho_{site} r_6 \quad (24)$$

Where ρ_{site} is the surface active site density with a unit of sites·cm^{-2}.

S2. The computational details of slow growth

To simulate the diffusion of oxygen, we positioned oxygen molecules approximately 5-6 Å away from the Pt surface (outside the HP), effectively mimicking the entire process of oxygen diffusing through the electric double layer and ultimately adsorbing onto the Pt catalyst surface.

The transformation from OO to H_2O involves the introduction of hydrogen atoms to form stable intermediates (*OOH, *O, *OH) and the confirmation of their structural stability. The initial state of each process is determined based on the stable structure obtained from the previous step, with the structure at the lowest energy point selected to ensure thermodynamic stability throughout each stage.

S3. The structure of Pt/ionomer/water interface

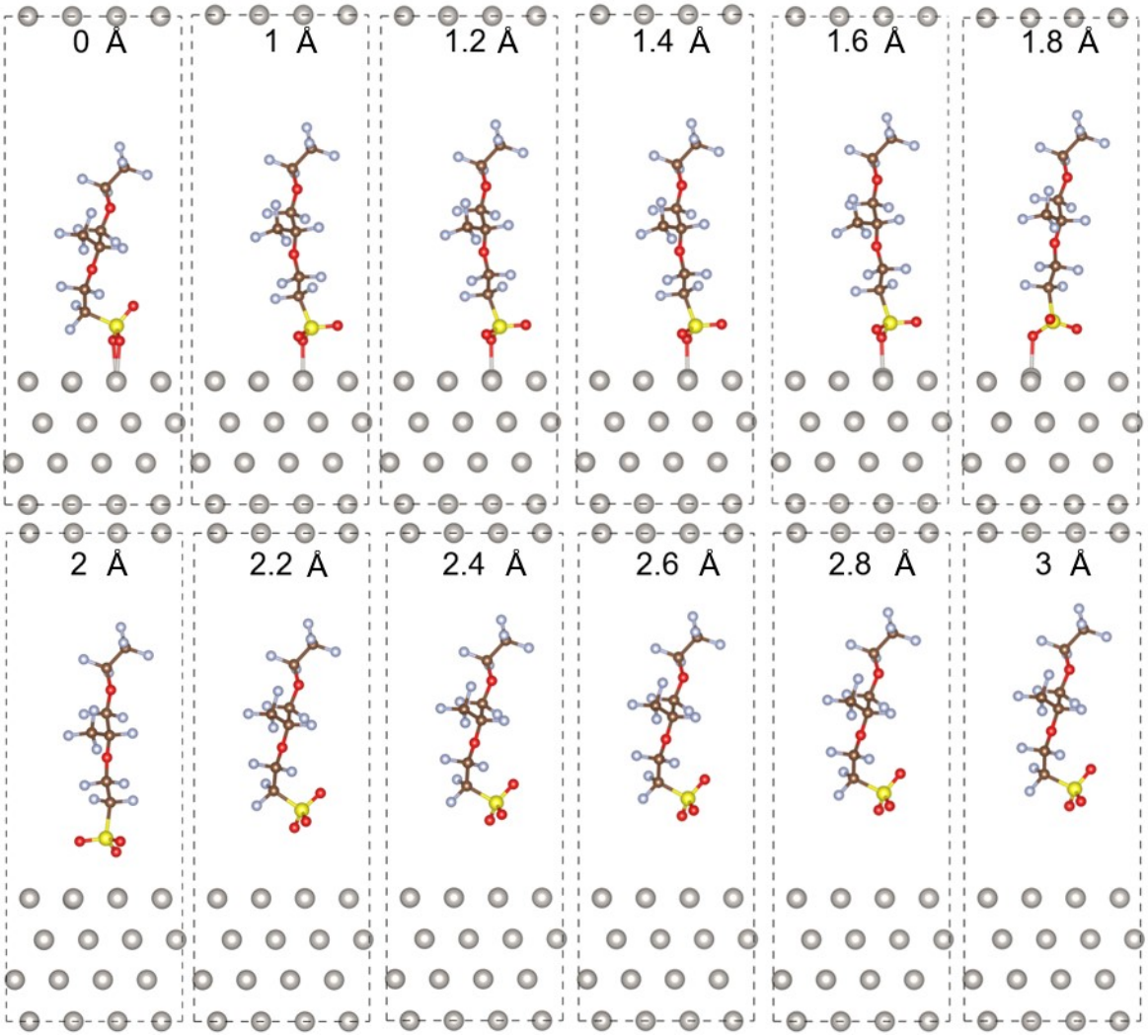

Fig. S1 Structures of the Pt(111)/Nafion ionomer interface with different distance.

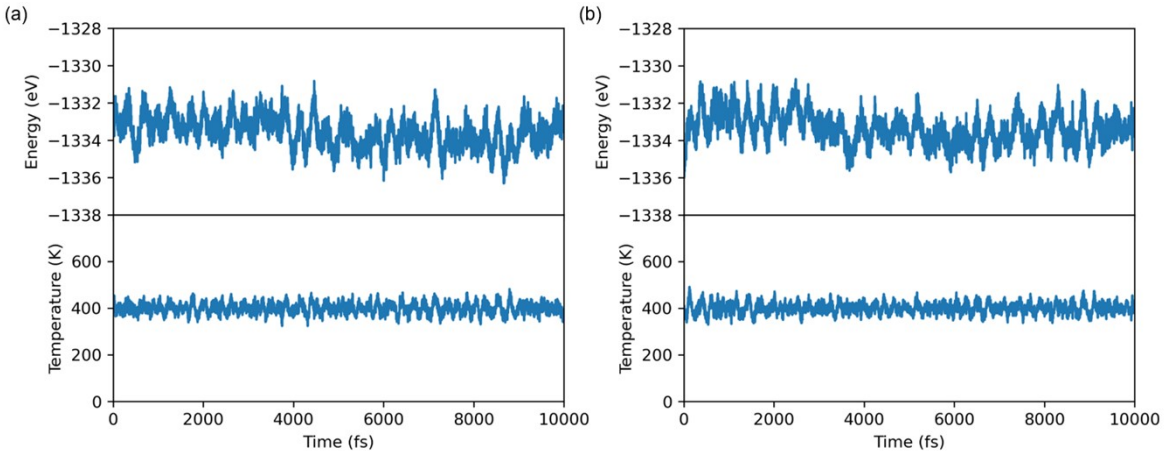

Fig. S2 Evolution of temperature and energy during a 10 ps AIMD simulation for the contact (a) and non-contact (b) structures.

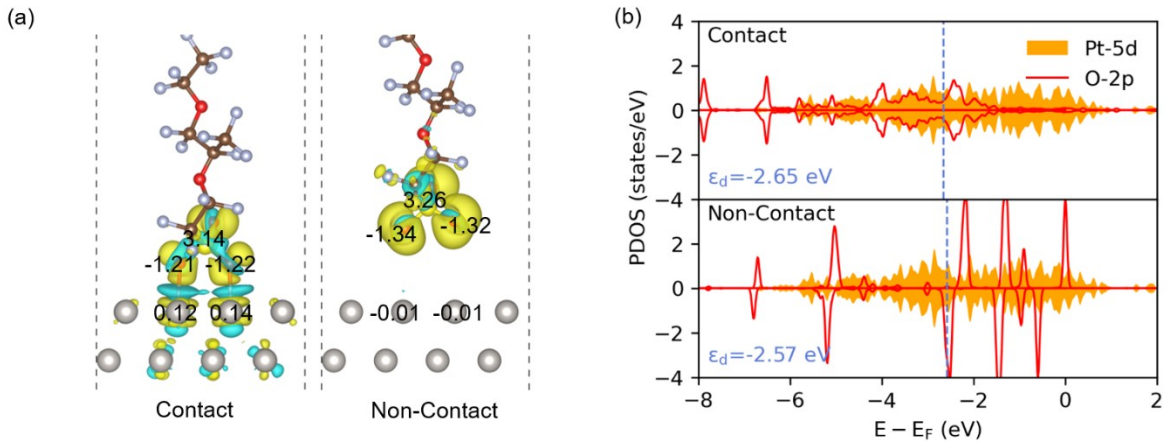

Fig. S3 (a) Differential charge density of the corresponding structures (iso-surface at 0.0003 e·Å^{-3}; cyan-green indicates electron deficiency, while yellow indicates electron accumulation) and Bader charge of atoms near the sulfonic acid group on the Pt surface; (b) PDOS of surface Pt atoms and O atoms of sulfonic acid groups, along with the d-band center in both contact and non-contact structures.

S4. The electric double-layer structure of the Pt/ionomer/water interface

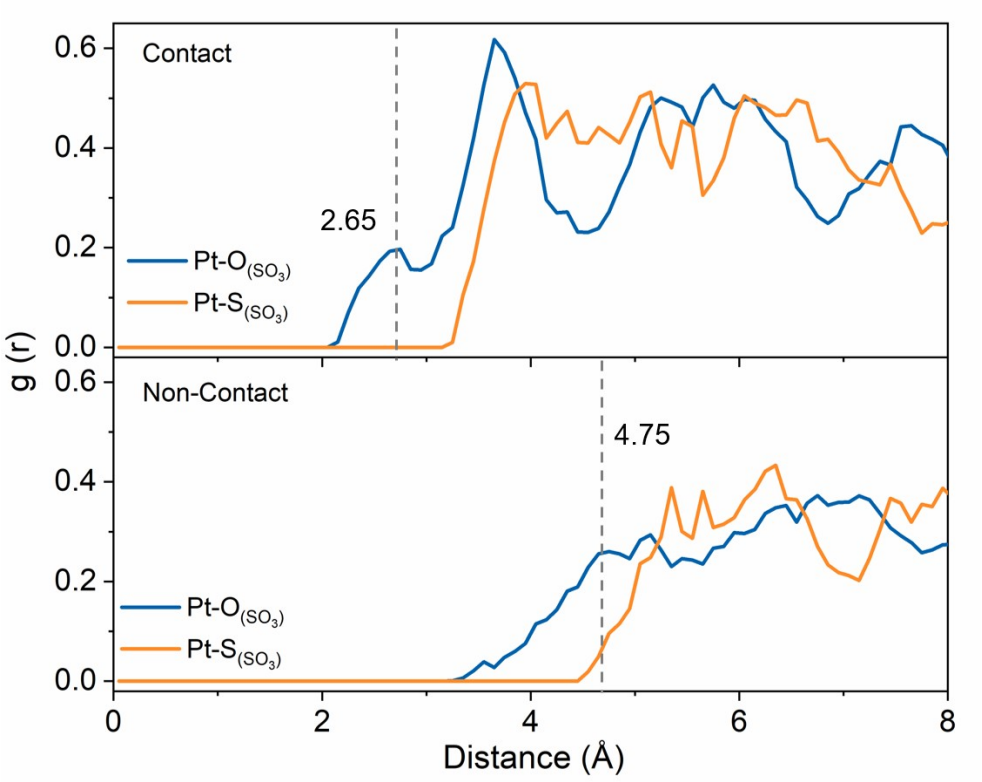

Fig. S4 RDF of Pt-O(SO_3) and Pt-S(SO_3) in both contact and non-contact structures.

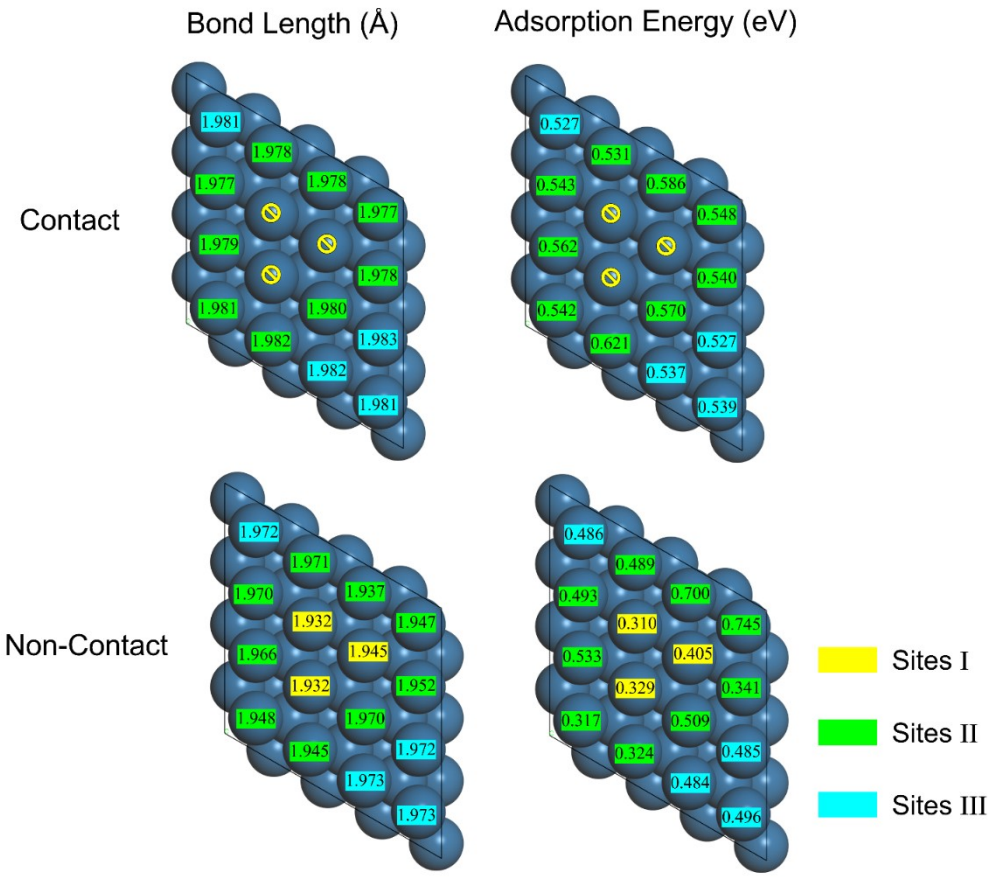

Fig. S5 Pt-OH bond lengths and adsorption energies of OH at various sites in both contact and non-contact structures. (The formula for calculating OH adsorption energies is $E_{ads}=E_{Pt/Nafion+OH}-E_{Pt/Nafion}$(after deformation)-$E_{H2O}-1/2E_{H2}$)

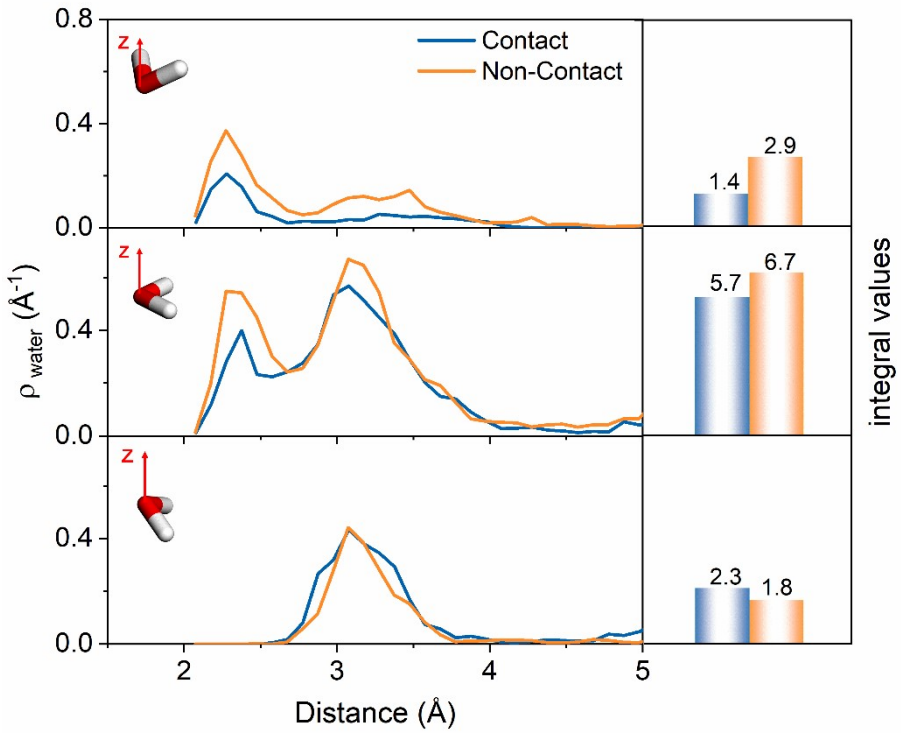

Fig. S6 Number density distribution and integral values of water within the HP, considering different orientation angles in both contact and non-contact structures.

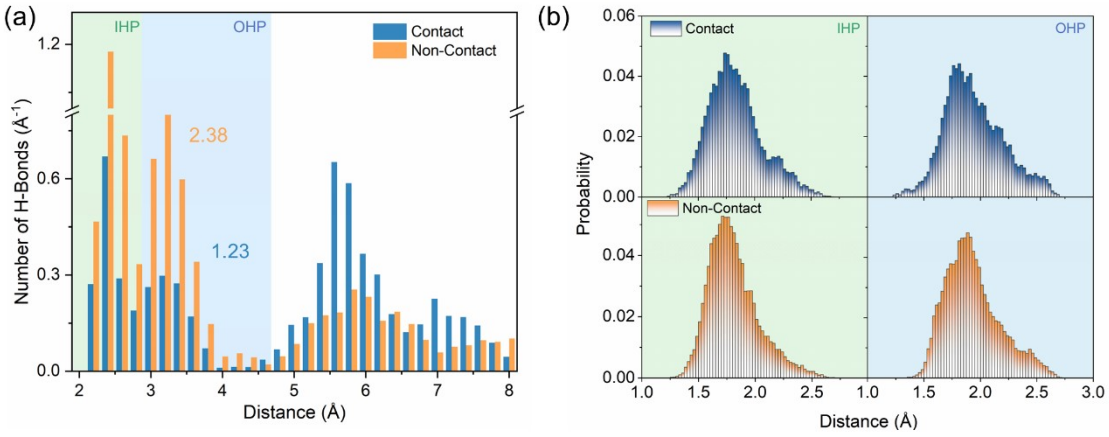

Fig. S7 The distribution of H-bond number density (a) and hydrogen bond length (b) (The values 1.23 and 2.38 represent the number of H-bonds within the HP in the contact and non-contact structures)

S5. The ORR activity of Pt/ionomer/water interface

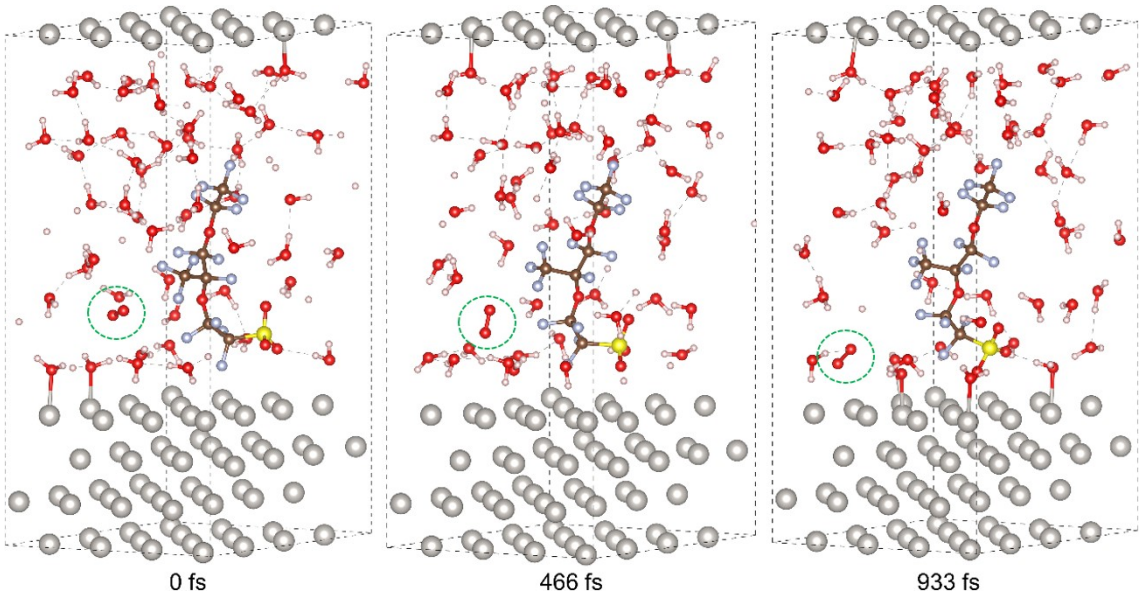

Fig. S8 Snapshots from the slow growth simulation of O_2 diffusion in the contact structure.

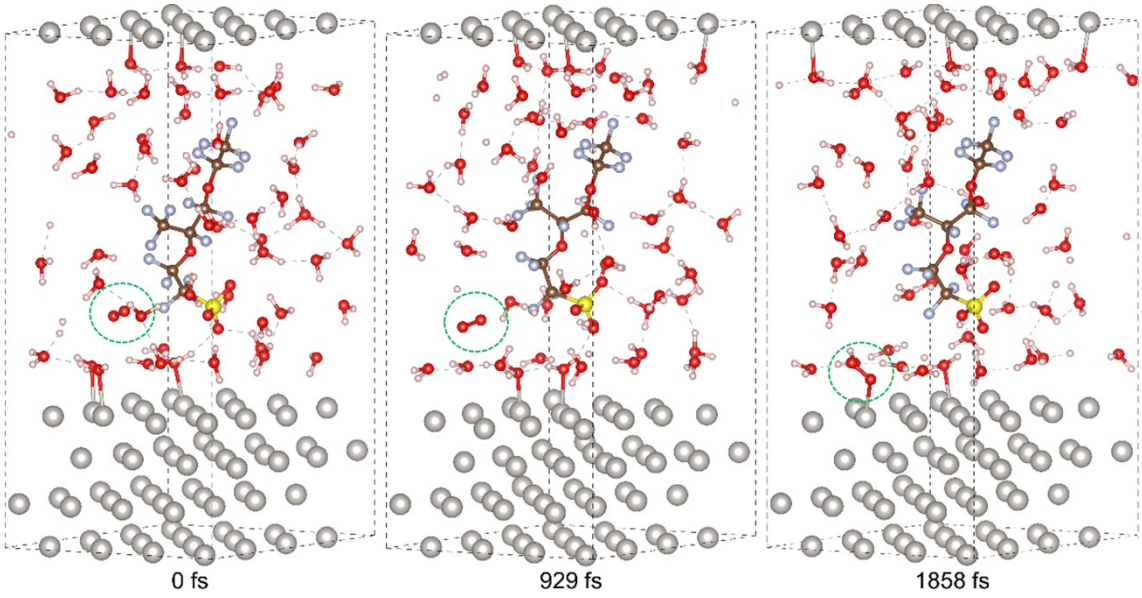

Fig. S9 Snapshots from the slow growth simulation of O_2 diffusion in the non-contact structure.

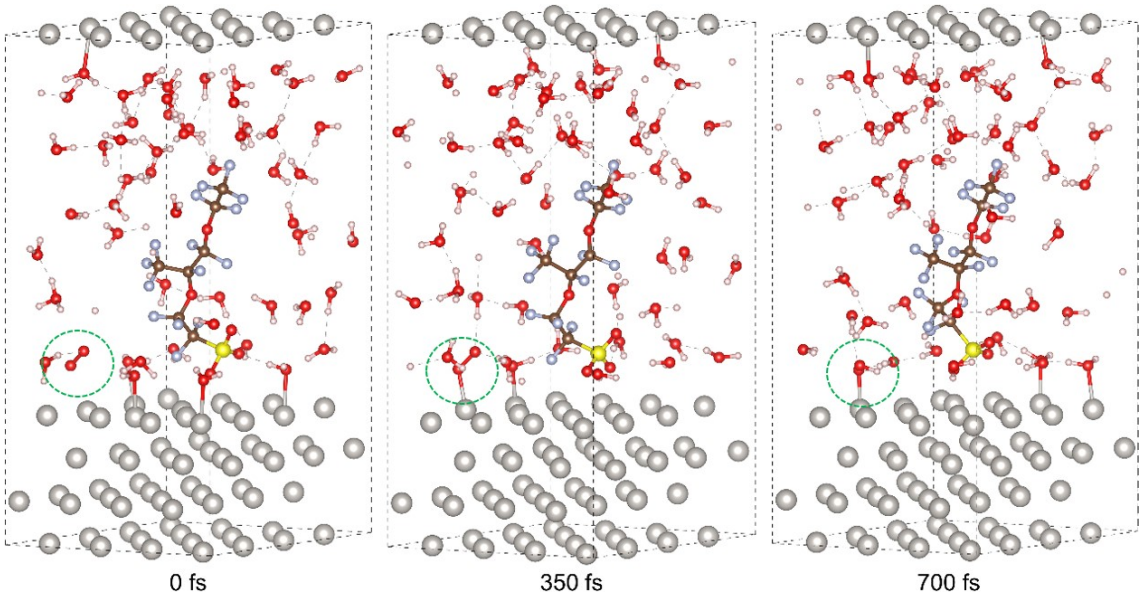

Fig. S10 Snapshots from the slow growth simulation of O_2 protonation (*OO + H^+ + e^- → *OOH) in the contact structure.

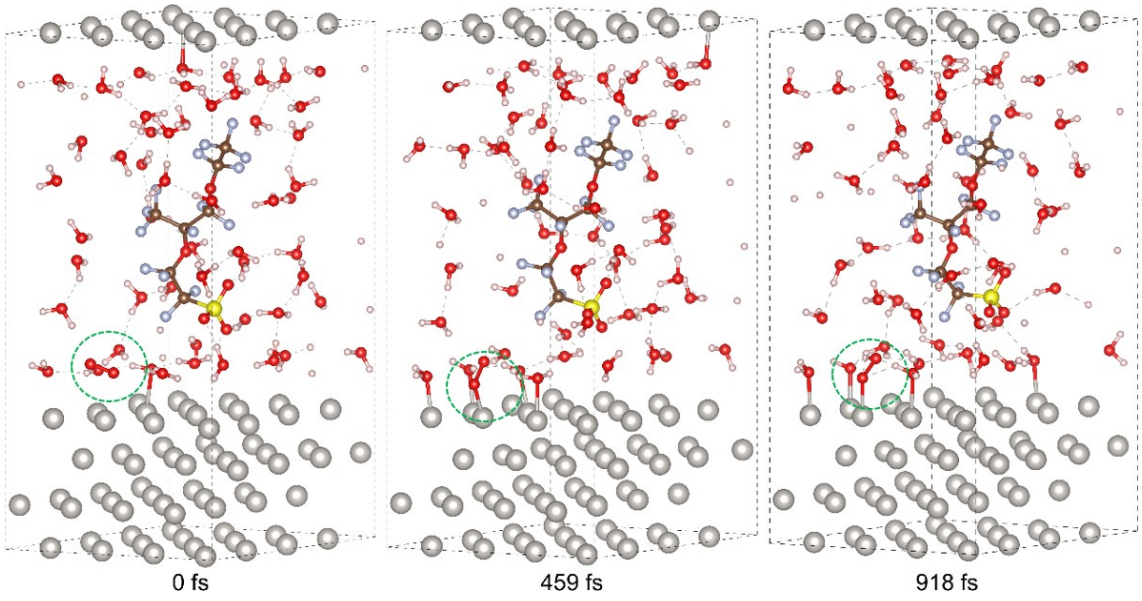

Fig. S11 Snapshots from the slow growth simulation of O_2 protonation (*OO + H^+ + e^- → *OOH) in the non-contact structure.

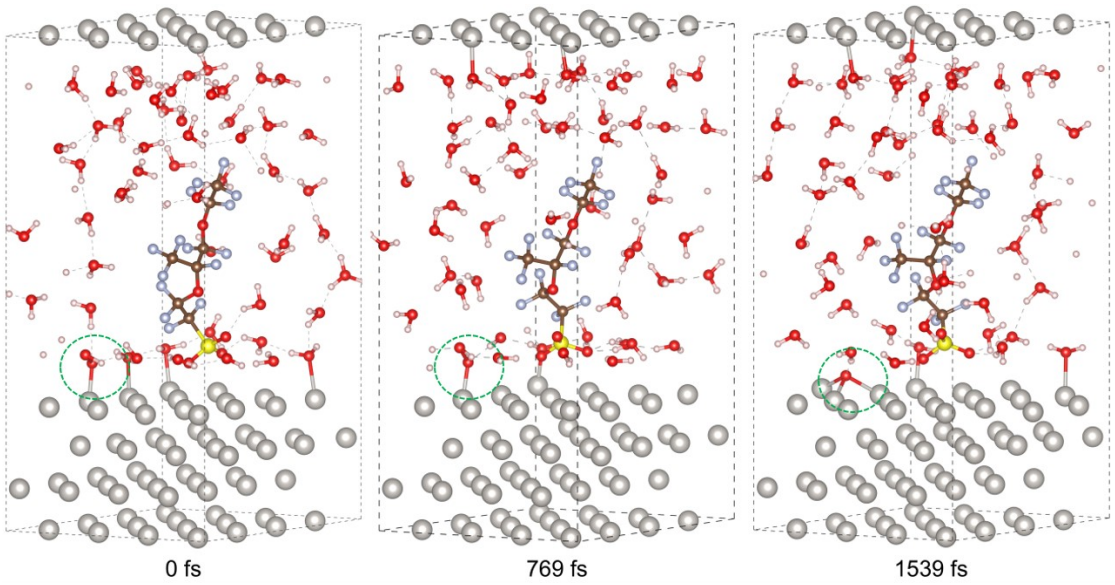

Fig. S12 Snapshots from the slow growth simulation of *OOH protonation (*OOH + H^+ + e^- → *O + H_2O) in the contact structure.

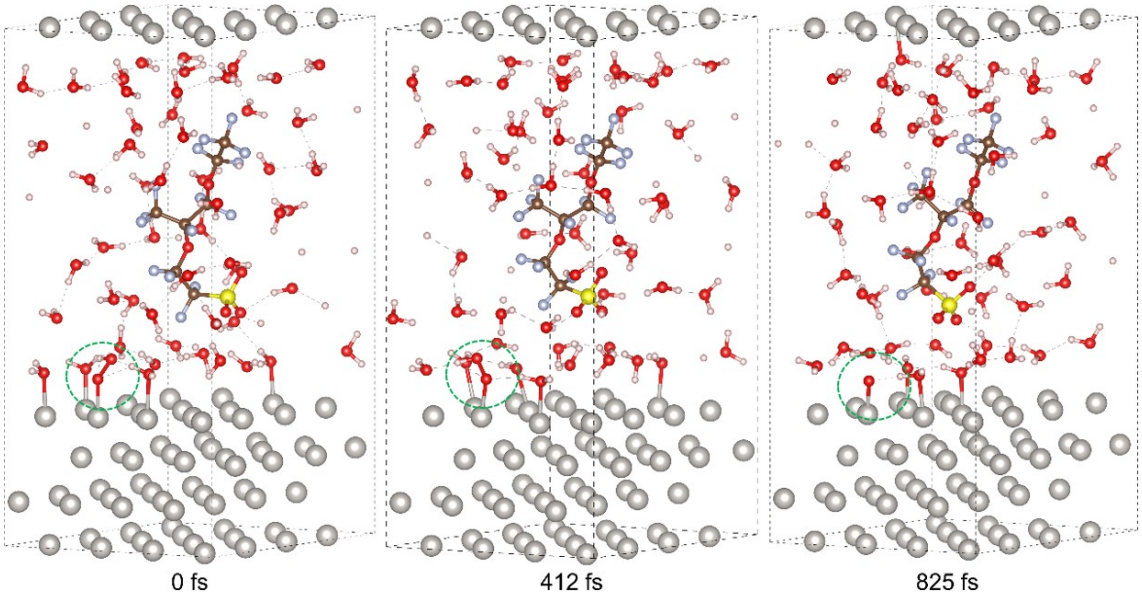

Fig. S13 Snapshots from the slow growth simulation of *OOH protonation (*OOH + H^+ + e^- → *O + H_2O) in the non-contact structure.

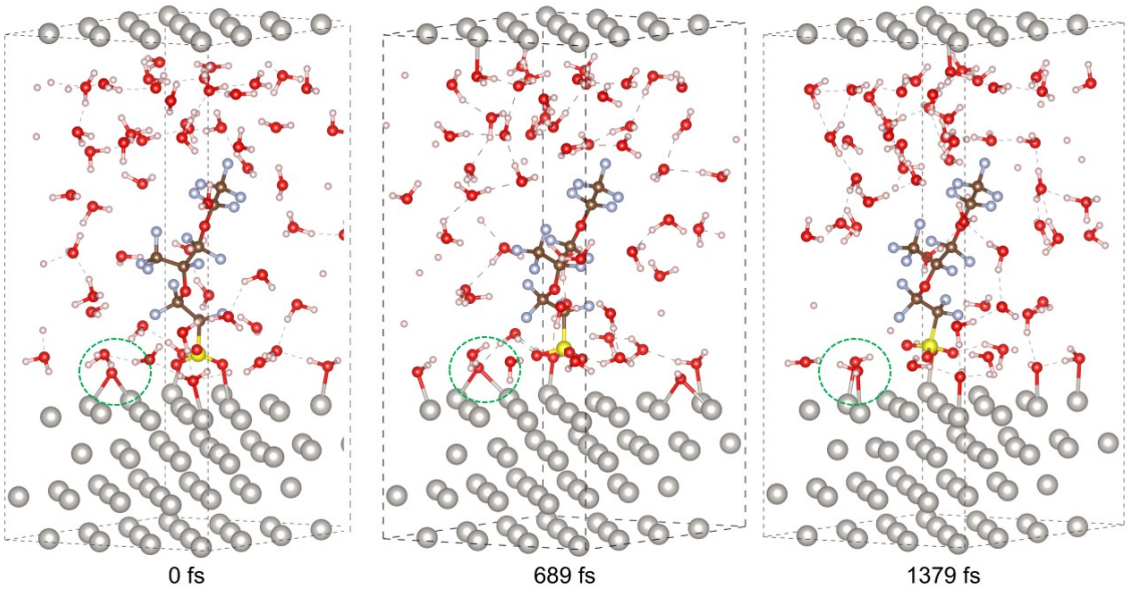

Fig. S14 Snapshots from the slow growth simulation of *O protonation (*O + H^+ + e^- → *OH) in the contact structure.

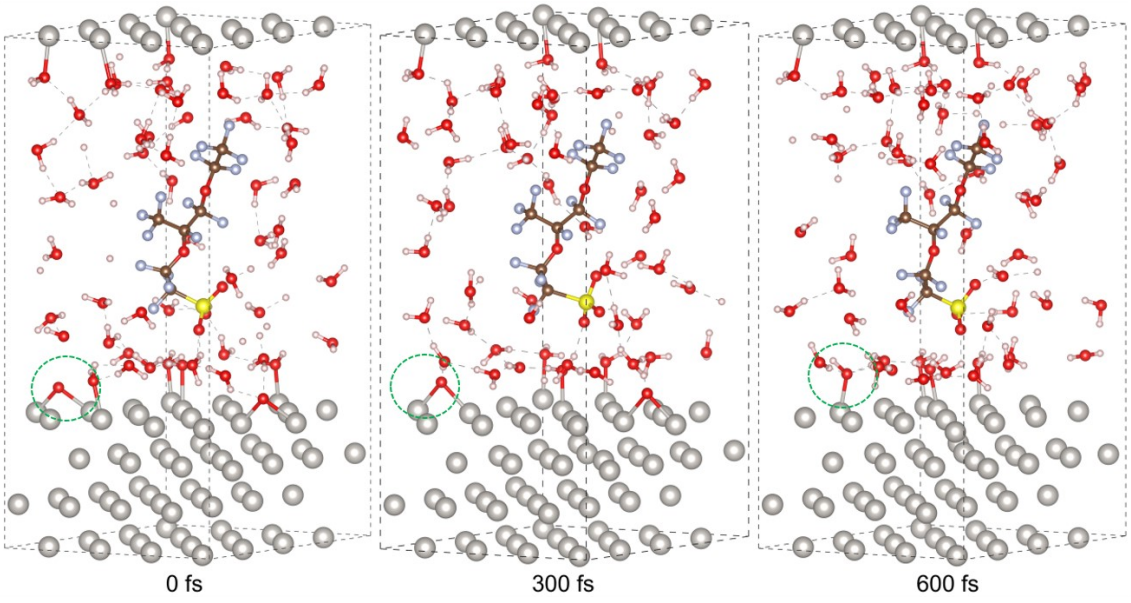

Fig. S15 Snapshots from the slow growth simulation of *O protonation (*O + H^+ + e^- → *OH) in the non-contact structure.

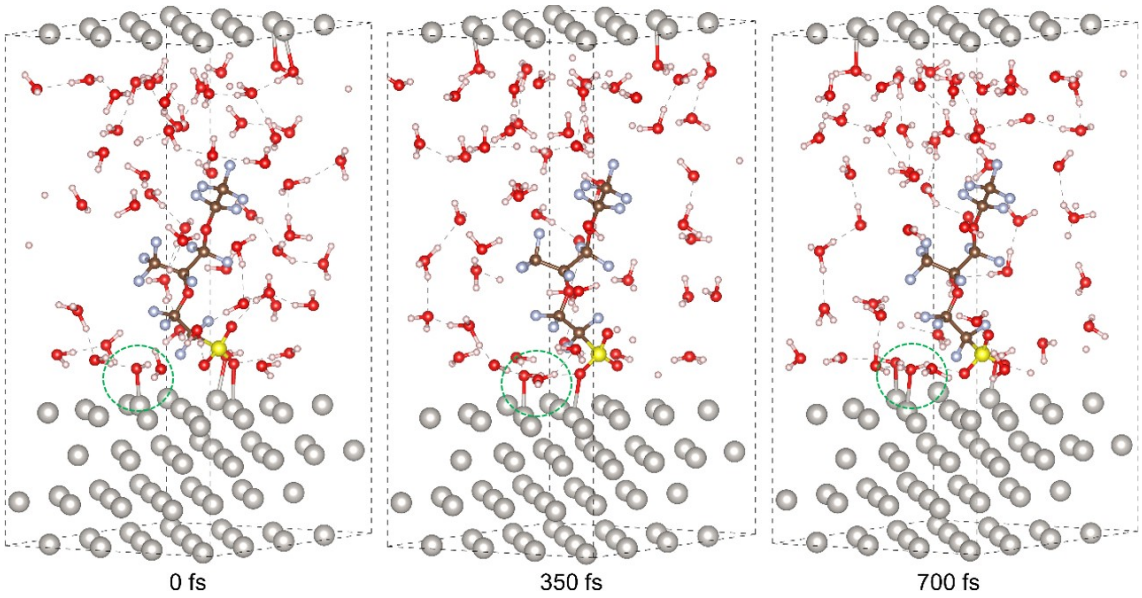

Fig. S16 Snapshots from the slow growth simulation of *OH protonation (*OH + H^+ + e^- → H_2O) in the contact structure.

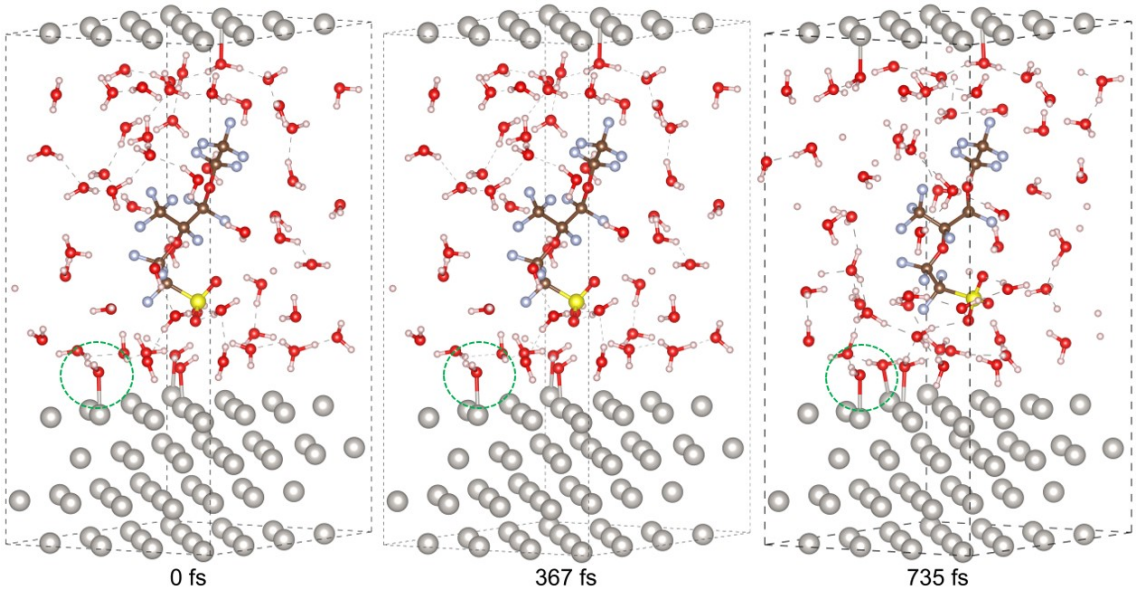

Fig. S17 Snapshots from the slow growth simulation of *OH protonation (*OH + H^+ + e^- → H_2O) in the non-contact structure.

Reference

1. H. A. Hansen, V. Viswanathan and J. K. Nørskov, Unifying Kinetic and Thermodynamic Analysis of 2 e^- and 4 e^- Reduction of Oxygen on Metal Surfaces, *J. Phys. Chem. C*, 2014, **118**, 6706-6718.
2. J. R. J.K. Norskov, A. Logadottir, L. Lindqvist, Origin of the Overpotential for Oxygen Reduction at a Fuel-Cell Cathode, *J. Phys. Chem. B*, 2004, **108**, 17886-17892.
3. V. Tripković, E. Skúlason, S. Siahrostami, J. K. Nørskov and J. Rossmeisl, The oxygen reduction reaction mechanism on Pt(111) from density functional theory calculations, *Electrochim. Acta*, 2010, **55**, 7975-7981.
4. L. C. Grabow, B. Hvolbæk, H. Falsig and J. K. Nørskov, Search Directions for Direct H_2O_2 Synthesis Catalysts Starting from Au_{12} Nanoclusters, *Top. Catal.*, 2012, **55**, 336-344.
5. D. C. Ford, A. U. Nilekar, Y. Xu and M. Mavrikakis, Partial and complete reduction of O_2 by hydrogen on transition metal surfaces, *Surf. Sci.*, 2010, **604**, 1565-1575.